

LETTER TO THE EDITOR

A Sample of [C II] Clouds Tracing Dense Clouds in Weak FUV Fields observed by Herschel[★]

J. L. Pineda, T. Velusamy, W. D. Langer, P. F. Goldsmith, D. Li., and H.W. Yorke

Jet Propulsion Laboratory, California Institute of Technology, 4800 Oak Grove Drive, Pasadena, CA 91109-8099, USA

Received / Accepted

ABSTRACT

The [C II] fine-structure line at $158\ \mu\text{m}$ is an excellent tracer of the warm diffuse gas in the ISM and the interfaces between molecular clouds and their surrounding atomic and ionized envelopes. Here we present the initial results from Galactic Observations of Terahertz C⁺ (GOTC⁺), a Herschel Key Project devoted to study the [C II] fine structure emission in the galactic plane using the HIFI instrument. We use the [C II] emission together with observations of CO as a probe to understand the effects of newly-formed stars on their interstellar environment and characterize the physical and chemical state of the star-forming gas. We collected data along 16 lines-of-sight passing near star forming regions in the inner Galaxy near longitudes 330° and 20° . We identify fifty-eight [C II] components that are associated with high-column density molecular clouds as traced by ^{13}CO emission. We combine [C II], ^{12}CO , and ^{13}CO observations to derive the physical conditions of the [C II]-emitting regions in our sample of high-column density clouds based on comparison with results from a grid of Photon Dominated Region (PDR) models. From this unbiased sample, our results suggest that most of [C II] emission originates from clouds with H₂ volume densities between $10^{3.5}$ and $10^{5.5}\ \text{cm}^{-3}$ and weak FUV strength ($\chi_0 = 1 - 10$). We find two regions where our analysis suggests high densities $> 10^5\ \text{cm}^{-3}$ and strong FUV fields ($\chi_0 = 10^4 - 10^6$), likely associated with massive star formation. We suggest that [C II] emission in conjunction with CO isotopes is a good tool to differentiate between regions of massive star formation (high densities/strong FUV fields) and regions that are distant from massive stars (lower densities/weaker FUV fields) along the line-of-sight.

Key words. ISM: atoms — ISM: molecules — ISM: structure

1. Introduction

The study of the processes governing the formation and destruction of molecular clouds is critical for our understanding of how galaxies have evolved in our Universe. In terms of column and local volume densities only two extreme states of cloud evolution have been systematically observed: diffuse atomic clouds traced by the 21 cm line of H I (e.g. Kalberla & Kerp 2009) and dense molecular clouds traced by rotational transitions of CO (e.g. Dame et al. 2001). We know, however, very little about the intermediate phases of cloud evolution and the interface between diffuse and dense molecular gas.

Galactic Observations of Terahertz C⁺ (GOTC⁺), a Herschel Key Project, is devoted to study the [C II] emission in different environments in our Galaxy. The survey will observe the [C II] $158\ \mu\text{m}$ line over a volume weighted sampling of 500 lines-of-sight (LOS). Upon completion, it will provide a database of a few thousand [C II]-emitting clouds distributed over the entire Galactic plane.

The [C II] fine structure line at $158\ \mu\text{m}$ is an excellent tracer of the interface between diffuse and dense molecular gas. The densities and temperatures in this interface allow effective collisional excitation of this line. The H I and H₂ volume densities are a significant fraction of, or comparable to, the critical den-

sities for collisional excitation¹ (3.3×10^3 and $7.1 \times 10^3\ \text{cm}^{-3}$ at $T = 100\ \text{K}$, respectively), the kinetic temperatures are $\sim 100\ \text{K}$, and the formation of CO is inhibited by limited shielding against far-ultraviolet (FUV) photons and therefore most of the gas-phase carbon is in C⁺ and some C⁰.

Here we present the first results on the molecular cloud-atomic cloud interface from the GOTC⁺ project. During the Herschel Priority Science and Performance Verification phase, we have collected data along 5 LOSs near $l = 340^\circ$ and 9 LOSs near $l = 20^\circ$ (Velusamy et al. 2010). The focus of this letter is to study [C II] components towards clouds that have sufficient column density to have significant ^{13}CO emission. Such regions can be considered as dense Photon-Dominated Regions (or photodissociation regions, or PDRs). PDRs are regions where the chemistry and thermal balance is dominated by the effects of FUV photons from young stars (Hollenbach & Tielens 1999, and references therein). These data are therefore important for the study of the stellar feedback of newly formed massive stars in their progenitor molecular cloud. We combine the [C II] data with observations of ^{12}CO and ^{13}CO from the ATNF Mopra 22-m telescope to study 58 high-column density PDRs. We use the [C II]/ ^{12}CO and [C II]/ ^{13}CO integrated intensity ratios to constrain physical conditions of the line-emitting gas comparing with a grid of PDR models.

¹ Electrons are a possibly significant collision partner of C⁺. However, the critical electron density for these particles to produce significant [C II] emission is $9.2\ \text{cm}^{-3}$ at $T = 100\ \text{K}$. The density in diffuse regions where the abundance relative to H is $X(e) \simeq X(\text{C}^+) \simeq 10^{-4}$ is modest ($\sim 10^2\ \text{cm}^{-3}$), while in the denser regions the ionization is significantly lower. In either case, the excitation by electrons is negligible.

Send offprint requests to: J. L. Pineda e-mail: Jorge.Pineda@jpl.nasa.gov

[★] Herschel is an ESA space observatory with science instruments provided by European-led Principal Investigator consortia and with important participation from NASA.

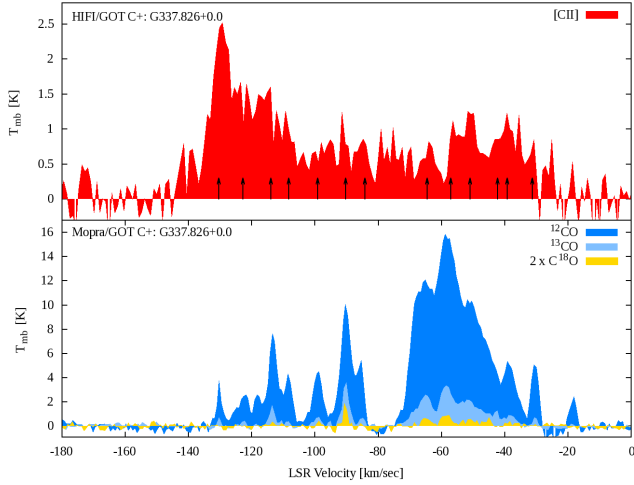


Fig. 1. [C II], ^{12}CO , ^{13}CO , and C^{18}O spectra towards the line-of-sight G337.826+0.0. The arrows indicate the [C II] components that have ^{13}CO counterparts.

The Galactic plane has been studied in [C II] with low velocity and spatial resolution observations with COBE (Bennett et al. 1994) and BICE (Nakagawa et al. 1998). The high angular ($12''$) and velocity (0.2 km s^{-1}) resolution of the Herschel/HIFI observations allow us to study for the first time the rich structure of molecular clouds along the line-of-sight towards the galactic plane. The Kuiper Airborne Observatory allowed the study of a handful of H II regions with velocity resolved [C II] observations (e.g. Boreiko et al. 1988; Boreiko & Betz 1991). However, they were limited to massive star-forming regions with dense and hot PDRs. The sensitivity of our observations allow us to study for the first time the population of PDRs in our galaxy that are exposed to weaker FUV radiation fields.

2. Observations

2.1. Herschel Observations

We observed the [C II] $^2\text{P}_{3/2} \rightarrow ^2\text{P}_{1/2}$ line at 1900.5469 GHz towards 16 LOSs in the Galactic plane with the HIFI (de Graauw et al. 2010) instrument on board the Herschel space observatory (Pilbratt et al. 2010). We refer to Velusamy et al. (2010) for more details about the [C II] observations. In Figure 1 we show sample LOS spectra of [C II], ^{12}CO , ^{13}CO , and C^{18}O .

2.2. Mopra Observations

We observed the $J = 1 \rightarrow 0$ transitions of ^{12}CO , ^{13}CO , and C^{18}O toward the observed [C II] LOSs. These observations are part of a survey of all GOT C+ positions towards the inner Galaxy between $l = -175.5^\circ$ and $l = 56.8^\circ$ conducted at the ATNF Mopra Telescope. The angular resolution of these observations is $33''$. Typical system temperatures were 600, 300, and 250 K for ^{12}CO , ^{13}CO , and C^{18}O , respectively. To convert from antenna to main-beam temperature scale we use a main-beam efficiency of 0.42 (Ladd et al. 2005). All lines were observed simultaneously using the MOPS spectrometer in zoom mode. The spectra were smoothed in velocity to 0.8 km s^{-1} for ^{12}CO and ^{13}CO and to 1.6 km s^{-1} for C^{18}O . Typical rms noise is 0.6 K for ^{12}CO and 0.1 K for both ^{13}CO and C^{18}O . We checked pointing accuracy every 60 minutes using the closest and brightest SiO maser.

3. [C II] components associated with molecular clouds

We identify a total of 146 [C II] velocity components in the observed LOSs. From this data set we identify components that are associated with high-column density molecular gas by looking for ^{13}CO counterparts. We identified most of the high- ^{13}CO column density [C II] components by fitting Gaussian functions defined by fitting the corresponding ^{13}CO spectra. The only exception was G337.826+0.0 for which we calculated the integrated intensity by determining the area within the FWHM of the ^{13}CO emission, as this line-of-sight shows complex velocity structure. Based on the ^{13}CO line parameters we identify 58 [C II] components associated with dense molecular gas. All of them also show ^{12}CO emission while 12 show C^{18}O emission. The remaining diffuse atomic and/or diffuse molecular [C II]-emitting clouds that do not have ^{13}CO counterparts are discussed by Langer et al. (2010) and Velusamy et al. (2010).

In the left panel of Figure 2, we summarize the observed characteristics by plotting the [C II]/ ^{12}CO and [C II]/ ^{13}CO integrated intensity ratios for the identified components as a function of the [C II] integrated intensity. The ratios are calculated from integrated intensities in units of K km s^{-1} . The mean value and standard deviation are 0.29 and 0.6 for the [C II]/ ^{12}CO integrated intensity ratio and 1.75 and 2.54 for [C II]/ ^{13}CO . The ratios vary over 2 orders of magnitude suggesting a wide range of physical conditions in our sample.

We use the [C II]/ ^{12}CO and [C II]/ ^{13}CO integrated intensity ratios to constrain the physical conditions of the line-emitting gas. The ^{12}CO emission, which becomes optically thick quickly after a modest fraction of the gas-phase carbon is converted to CO, is not very sensitive to the FUV radiation field, as the temperature at the $\text{C}^+/\text{C}^0/\text{CO}$ transition layer is also insensitive to this quantity (Wolfire et al. 1989; Kaufman et al. 1999). Therefore, the [C II]/ ^{12}CO ratio is determined by the column density of C^+ and the temperature at the surface of the PDR, which are in turn dependent on the FUV radiation field and H_2 density. The [C II]/ ^{13}CO ratio is proportional to the ratio between the C^+ and ^{13}CO column densities. It therefore gives, provided that extra constraints on the total column of material are available and that there are no significant variations of the FUV field within the beam, a constraint on the location of the $\text{C}^+/\text{C}^0/\text{CO}$ transition layer which in turn depends on the strength of the FUV field and H_2 density.

4. Comparison with PDR model calculations

We compare the observed [C II]/ ^{12}CO and [C II]/ ^{13}CO integrated intensity ratios with the results of a PDR model grid in order to constrain physical conditions of the [C II]-emitting clouds.

The model grid was calculated using the KOSMA- τ PDR model (Störzer et al. 1996; Röllig et al. 2006) which is available online². The model provides a self-consistent solution of the chemistry and thermal balance of a spherical cloud, with a truncated density profile, which is illuminated isotropically by a FUV radiation field. The density distribution has the form, $n(r) = n_s(r/r_c)^{-1.5}$ for $0.2r_c \leq r \leq r_c$ and a constant density of $n(r) = n_s(0.2)^{-1.5}$ in the central region of the cloud ($r < 0.2r_c$). Here r_c is the cloud radius and n_s is the density at the cloud surface. Note that with a power-law index of 1.5, the average density of the clump is about twice the density at the cloud surface. The line intensities are calculated using a non-LTE radi-

² <http://hera.ph1.uni-koeln.de/~pdr/>

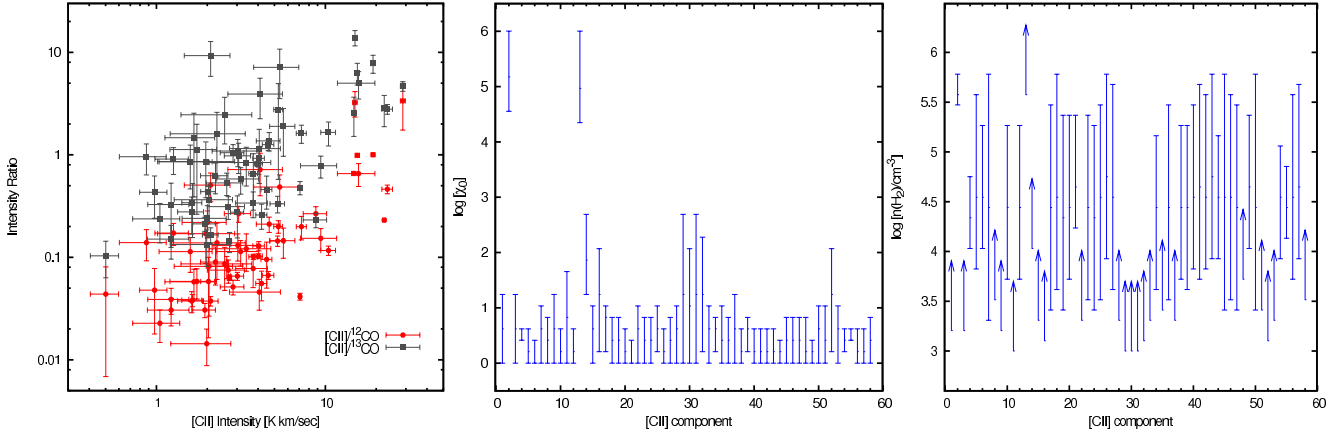


Fig. 2. (*left panel*) The observed [C II]/¹²CO and [C II]/¹³CO integrated intensity ratios for our sample of [C II] components associated with high-column density molecular clouds. The ratios are calculated from integrated intensities in units of K km s⁻¹. The horizontal error bars are the uncertainties in the determination of the [C II] integrated intensities. The vertical error bars are the uncertainties in the line ratios which are derived from error propagation. (*central and right panels*) Results of the comparison between [C II]/¹²CO and [C II]/¹³CO ratios for all identified [C II] components and the PDR model grid showing the constrained ranges in FUV radiation field (*central panel*) and H₂ volume density (*right panel*). The arrows indicate lower limits to the H₂ volume density.

tive transfer code by Gierens et al. (1992). Each model is characterized by the clump mass, the density at the cloud surface, and strength of the FUV field. The clump mass ranges from 10⁻² to 100 M_⊙, the density at the cloud surface from 10³ to 10⁶ cm⁻³, and the strength of the FUV field from $\chi_0 = 1$ to 10⁶ (in units of the Draine 1978 field³). We do not use H I and C¹⁸O observations to constrain our solutions as model grids involving their emission are not available.

By using a spherically symmetric model we assume that the cloud spatial structure can be described by an ensemble of clumps with sizes much smaller than the resolution of our observations. Additionally, we assume that each clump in this ensemble has the same mass and density, and that the [C II]/¹²CO and [C II]/¹³CO line ratios can be estimated using the line ratios of a single clump of that mass and density. Therefore, the comparison with the PDR model grid provides the typical incident FUV field, mass, and density of the regions that dominate the observed line ratios. An even more realistic model considers clumps following the distribution of masses and sizes observed in many molecular clouds (e.g. Zielinsky et al. 2000; Cubick et al. 2008).

The central and right panels in Figure 2 show a summary of the constrained H₂ volume densities and FUV radiation fields for our sample. We consider models with chi-squared χ^2 smaller than $1.1\chi_{\min}^2$. We find two [C II] components with high volume densities (> 10⁵ cm⁻³) and strong FUV fields (between $\chi_0 = 10^4 - 10^6$). Both regions are characterized by [C II]/CO integrated intensity ratios that are larger than 1 (c.f. Orion has a [C II]/¹²CO ratio of 1.36; Crawford et al. 1985). We show an image and [C II] spectrum of one such source in Figure 3. The remaining components have lower volume densities between 10^{3.5} - 10^{5.5} cm⁻³. Six of those could have a strength of FUV field as high as 100 while the majority (51 components) have FUV fields between 1 and 10. For all components the comparison with the PDR model grid suggests clump masses that are larger than 1 M_⊙. Note that

³ The average FUV intensity of the local ISM is 2.2×10^{-4} erg cm⁻² s⁻¹ sr⁻¹ (Draine 1978). Note that the Draine field is isotropic (i.e. a given point is illuminated from 4 π steradians) while the surface of the clouds considered here are only illuminated from 2 π steradians. Therefore the rate of photoreactions at the cloud surface are half of what they would be with the Draine field in free space.

due to the limited spatial coverage of the observations presented here, the distribution of physical conditions is not smooth. We will obtain a much better sampling of the distribution of physical conditions in velocity components distributed over the entire galactic plane with the completed **GOT C+** survey.

The large number of components with low-FUV field is a result of the low observed [C II]/¹²CO ratios of about 0.1. Such values of the [C II]/¹²CO ratio are expected for $\chi_0 < 10^3$ over a large range of H₂ volume densities (see e.g. Figure 9 in Kaufman et al. 1999). The [C II]/¹³CO ratio provides an additional constraint on the FUV field. The majority of the observed components have small ratios that suggest a large column density of ¹³CO relative to that of C⁺. This result is suggestive of a C⁺/C⁰/CO transition occurring close to the surface of the cloud which is a result of either high densities or weak FUV fields. Note, however, that using [C II] and ¹³CO to constrain the location of the C⁺/C⁰/CO transition requires extra constraints on the total column density of material throughout the clump which in turn depends on the assumed clump surface density and mass. These two quantities are not well constrained in the analysis presented here. Additionally, it requires that there are no significant variations of the FUV field within the beam as shielded clumps might contribute significantly to the ¹³CO emission but little to that of [C II]. The H₂ volume density for individual velocity components can be better determined using observations of the 609 μ m and 370 μ m transitions of neutral carbon, which have been used to constrain the temperature and density at the C⁺/C⁰/CO transition region in PDRs (e.g. Stutzki et al. 1997). The [C II] to bolometric infrared flux is also useful to constrain the FUV field (Wolfire et al. 1989; Kaufman et al. 1999) but is only useful towards LOSs with a single velocity component.

5. Discussion

We have found that most of the [C II] velocity components considered here are associated with regions that are exposed to weak FUV radiation field ($\chi_0 < 10$) and therefore are away from OB associations. PDRs exposed to weak FUV radiation fields have been studied in a few sources using [C I] emission (e.g. Maezawa et al. 1999; Bensch 2006; Pineda & Bensch

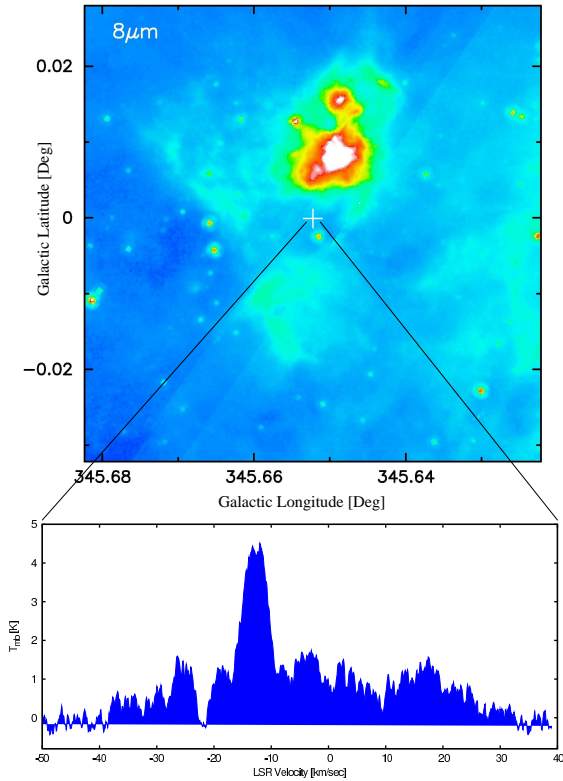


Fig. 3. Example of [C II] emission associated with a massive star forming region. The line-of-sight G345.65+0.0 passes near several bright H II regions as shown in the Spitzer $8\mu\text{m}$ image. In this line-of-sight we find a bright [C II] velocity component at -12.9 km s^{-1} which our analysis suggests arises from a region with high density ($\sim 10^{5.7}\text{ cm}^{-3}$) and strong FUV field ($\chi_0 = 10^{4.5} - 10^6$).

2007) but never observed with velocity-resolved [C II] before Herschel/HIFI.

Cubick et al. (2008) suggested that most of the [C II] in our Galaxy originates from a clumpy medium exposed to a FUV field of $\chi_0 = 10^{1.8}$, which is larger than the upper limit determined for the majority of the observed components. Note, however, that their model does not consider emission arising from diffuse clouds. From our observed LOSs, we find that about 56% of the total detected [C II] emission arises from low-column density regions (without significant ^{13}CO emission; Langer et al. 2010; Velusamy et al. 2010) while 44% is emitted from dense PDRs. Nevertheless, the moderate FUV field predicted by Cubick et al. (2008) might suggest that the predominance of low-FUV radiation field regions observed in our limited sample (covering less than 2% of the entire GOT C+ survey) might hold for the entire Galaxy.

We found two regions where our analysis suggests high densities ($> 10^5\text{ cm}^{-3}$) and strong FUV fields (between $\chi_0 = 10^4$ and 10^6). These regions are likely associated with massive star formation. This conclusion is a result of the elevated [C II]/CO ratio observed towards these regions. This identification suggests that the [C II]/CO ratio is good tracer of the location of massive star formation regions in the galaxy. [C II] observations will therefore provide an alternative method to determine the distribution of massive star forming regions in the galaxy (e.g. Bronfman et al. 2000). Note that velocity resolved observations are crucial for the interpretation of the [C II]/CO ratio. In our observed LOSs

we have found velocity components showing [C II] emission but no CO as well as components showing CO but no [C II]. Velocity unresolved observations would have given a distorted value of the [C II]/CO ratio that would result in an incorrect interpretation of the physical conditions of the line-emitting gas.

6. Conclusions

We have presented velocity-resolved observations of [C II] towards 16 LOSs located near $l = 340^\circ$ and $l = 20^\circ$ in the Galactic plane using the HIFI instrument on board the Herschel space observatory. We identified a total of 146 different [C II] velocity components. In this letter we analyzed a sample of 58 components that are associated with high-column density molecular gas as traced by ^{13}CO emission. These components contribute 44% of the total observed [C II] emission implying a significantly larger amount of [C II] emission originating in the diffuse ISM than from star forming environments. We have compared the [C II]/ ^{12}CO and [C II]/ ^{13}CO integrated intensity ratios with a PDR model grid to constrain the strength of the FUV field and the H_2 volume density in this sample. We find two clouds for which our analysis suggests high densities ($> 10^5\text{ cm}^{-3}$) and strong FUV fields ($\chi_0 = 10^4 - 10^6$), likely associated with massive star formation. The majority of the observed components, however, have modest densities ($10^{3.5} - 10^{5.5}\text{ cm}^{-3}$) and weaker FUV fields ($\chi_0 = 1 - 10$). Although the population of clouds with these conditions is likely where most of the [C II] emission originates in our Galaxy, their properties are largely unexplored. The GOT C+ survey will provide a few thousand clouds distributed in the Galactic plane and therefore will allow us to characterize this population of intermediate clouds.

Acknowledgements. We would like to thank the referee David Hollenbach for his comments and suggestions that significantly improved this letter. This work was performed by the Jet Propulsion Laboratory, California Institute of Technology, under contract with the National Aeronautics and Space Administration. We thank the staffs of the ESA and NASA Herschel Science Centers for their help. The Mopra Telescope is managed by the Australia Telescope, which is funded by the Commonwealth of Australia for operation as a National Facility by the CSIRO.

References

- Bennett, C. L., Fixsen, D. J., Hinshaw, G., et al. 1994, *ApJ*, 434, 587
- Bensch, F. 2006, *A&A*, 448, 1043
- Boreiko, R. T. & Betz, A. L. 1991, *ApJ*, 380, L27
- Boreiko, R. T., Betz, A. L., & Zmuidzinas, J. 1988, *ApJ*, 325, L47
- Bronfman, L., Casassus, S., May, J., & Nyman, L. 2000, *A&A*, 358, 521
- Crawford, M. K., Genzel, R., Townes, C. H., & Watson, D. M. 1985, *ApJ*, 291, 755
- Cubick, M., Stutzki, J., Ossenkopf, V., Kramer, C., & Röllig, M. 2008, *A&A*, 488, 623
- Dame, T. M., Hartmann, D., & Thaddeus, P. 2001, *ApJ*, 547, 792
- de Graauw, T., Helmich, F. P., Phillips, T. G., et al. 2010, *A&A*, 518, L6+
- Draine, B. T. 1978, *ApJS*, 36, 595
- Gierens, K. M., Stutzki, J., & Winnewisser, G. 1992, *A&A*, 259, 271
- Hollenbach, D. J. & Tielens, A. G. G. M. 1999, *Reviews of Modern Physics*, 71, 173
- Kalberla, P. M. W. & Kerp, J. 2009, *ARA&A*, 47, 27
- Kaufman, M. J., Wolfire, M. G., Hollenbach, D. J., & Luhman, M. L. 1999, *ApJ*, 527, 795
- Ladd, N., Purcell, C., Wong, T., & Robertson, S. 2005, *PASA*, 22, 62
- Langer, W. D., Velusamy, T., Pineda, J. L., et al. 2010, *ArXiv:1007.3048*
- Maetzawa, H., Ikeda, M., Ito, T., et al. 1999, *ApJ*, 524, L129
- Nakagawa, T., Yui, Y. Y., Doi, Y., et al. 1998, *ApJS*, 115, 259
- Pilbratt, G. L., Riedinger, J. R., Passvogel, T., et al. 2010, *A&A*, 518, L1+
- Pineda, J. L. & Bensch, F. 2007, *A&A*, 470, 615
- Röllig, M., Ossenkopf, V., Jeyakumar, S., Stutzki, J., & Sternberg, A. 2006, *A&A*, 451, 917
- Störzer, H., Stutzki, J., & Sternberg, A. 1996, *A&A*, 310, 592

- Stutzki, J., Graf, U. U., Haas, S., et al. 1997, *ApJ*, 477, L33+
- Velusamy, T., Langer, W. D., Pineda, J. L., et al. 2010, [ArXiv:1007.3338](https://arxiv.org/abs/1007.3338)
- Wolfire, M. G., Hollenbach, D., & Tielens, A. G. G. M. 1989, *ApJ*, 344, 770
- Zielinsky, M., Stutzki, J., & Störzer, H. 2000, *A&A*, 358, 723